Journal of Alloys and Compounds 514 (2012) 127–134

Contents lists available at SciVerse ScienceDirect

Journal of Alloys and Compounds

journal homepage: www.elsevier.com/locate/jallcom

First principles calculations of interstitial and lamellar rhenium nitrides

G. Soto*, H. Tiznado, A. Reyes[1], W. de la Cruz

Universidad Nacional Autónoma de México, Centro de Nanociencias y Nanotecnología, Km 107 Carretera Tijuana-Ensenada, Ensenada Baja California, Mexico

ARTICLE INFO

Article history:
Received 9 September 2011
Received in revised form 3 November 2011
Accepted 4 November 2011
Available online 26 November 2011

Keywords:
Nitride
Rhenium
Structure

ABSTRACT

We report here a systematic first principles study of two classes of variable-composition rhenium nitride: ***i***, interstitial rhenium nitride as a solid solution and ***ii***, rhenium nitride in lamellar structures. The compounds in class ***i*** are cubic and hexagonal close-packed rhenium phases, with nitrogen in the octahedral and tetrahedral interstices of the metal, and they are formed without changes to the structure, except for slight distortions of the unit cells. In the compounds in class ***ii***, by contrast, the nitrogen inclusion provokes stacking faults in the parent metal structure. These faults create trigonal-prismatic sites where the nitrogen residence is energetically favored. This second class of compounds produces lamellar structures, where the nitrogen lamellas are inserted among multiple rhenium layers. The Re_3N and Re_2N phases produced recently by high-temperature and high-pressure synthesis belong to this class. The ratio of the nitrogen layers to the rhenium layers is given by the composition. While the first principle calculations point to higher stability for the lamellar structures as opposed to the interstitial phases, the experimental evidence presented here demonstrates that the interstitial classes are synthesizable by plasma methods. We conclude that rhenium nitrides possess polymorphism and that the two-dimensional lamellar structures might represent an emerging class of materials within binary nitride chemistry.

1. Introduction

The binary nitrides formed by metals of the IV–VII groups of the periodic table are often classified as solid solutions [1,2]. The solid solution model requires that the crystal structure of the solvent, which in this case is the metal, must remain unchanged by the addition of the solute. Nitrogen is the solute, and the solvent–solute mixture remains a single homogeneous phase. This model considers that the dissolution occurs through the solute's occupation of empty spaces, or interstices, between the atoms of the solvent. These alloys can have a non-stoichiometric composition because the limiting factor is the available space for the dissolution of interstitials. Many of the interstitial nitrides have structures that are different from those of the associated metals and therefore deviate from the solid solution model. For example, titanium metal has a hexagonal close-packed structure, while its nitride, TiN, has a cubic close-packed structure. As the nitrogen atoms fill the interstitial sites, structural changes occur in the host metal. The concept of an interstitial solid solution is a coarse approximation for binary metal nitrides, valid only for small compositional variations or for a limited range of metal nitrides. More often, the structure of the parent metal changes upon the addition of nitrogen. The departure from the solid solution model is justified by the moderate electronegativity of nitrogen, which introduces a certain level of ionic character to the solid. Nitrogen becomes a negatively charged ion, and the repulsion between these charged species, which are covalently bonded to metal atoms, might induce changes in the host structure. For yttrium nitride, we have previously studied the structural conversion from the hexagonal metal to the cubic nitride by first principles calculations [3].

In this study, we investigate the rhenium nitride structures, ReN_x, as a function of x, for $x \leq 1$. Until now, the nitrides of group VII have been scantily studied both theoretically and experimentally. Rhenium nitrides have been synthesized by several methods, including laser ablation [4,5], high-pressure high-temperature anvil cell reaction [6], the reaction of rhenium pellets with ammonia at high temperature [7], ion implantation of nitrogen into a rhenium foil [8] and reactive DC-magnetron sputtering, as we present here in this work. From the few reports available on the topic, the rhenium nitrides are expected to have exceptional properties, such as very high bulk moduli, high hardness and brittleness [9,10], catalytic activity [7], and superconductivity [8,11]. These materials may have potential applications in hard coatings for cutting tools and in heterogeneous catalysis.

The goal of this study is to show that rhenium nitride might behave in a unique way as it is being nitrided. It exhibits polymorphism, but some polymorphs contain mono-atomic layers of nitrogen sandwiched among layers of rhenium. These layers of nitrogen (hexagonal rings) may influence the electronic properties

* Corresponding author at: CNyN-UNAM, P.O. Box 439036, San Ysidro, CA 92143-9036, USA. Tel.: +52 646 1744602; fax: +52 646 1744603.
E-mail address: gerardo@cnyn.unam.mx (G. Soto).
[1] A. Reyes is on a sabbatical leave at Department of Physics, The Pennsylvania State University, University Park, Pennsylvania 16802, USA.

0925-8388/$ – see front matter © 2011 Elsevier B.V. All rights reserved.
doi:10.1016/j.jallcom.2011.11.023

of the solids in a very interesting way. We will use terms like 'layered solutions' or 'lamellar structures' in the absence of a better phrase to describe the behavior of such compounds. Such solids are not new. They have been studied since 1975 in systems where carbon is contained in transition metals [12].

2. Rhenium nitrides as interstitial and lamellar structures

As mentioned above, transition metal nitrides are prejudged to be solid solutions. Therefore, most of the experimental diffraction patterns are interpreted accordingly. For example, ReN_x has been synthesized by the decomposition of $(NH_4)ReO_4$ in an NH_3-containing atmosphere [7,13] and by nitrogen-ion planting into Re metal [8]. Those studies reported fcc crystalline structures, for compositions from $x = 0.43$ to $x = 1$. In another report where rhenium nitride films were made by the pulsed laser deposition method, the resulting structures could be either cubic or hexagonal [5]. With a low nitrogen content, $x = 0.06$, the film maintained a Re-like hexagonal arrangement, while for $x = 0.17$ and $x = 0.22$, the films adopted cubic structures. The authors concluded that the hcp structure of metallic Re changed to a cubic structure with an increase in the number of nitrogen atoms occupying the interstitial sites between the Re atoms. From the above studies, we might conclude that the application of the interstitial-solid-solution model to rhenium nitrides is correct, as it maintains an fcc arrangement for large variations in nitrogen content.

Opposition to that conclusion may be found in the study reported by Friedrich et al. [6], in which rhenium nitride was synthesized by the high-pressure high-temperature method and the structure was obtained by Rietveld refinements and density functional theory optimizations. Two hexagonal phases were proposed to explain the authors' diffraction experiments. None of these phases coincides with the structures obtained by the methods of the above paragraph, although their compositions are equivalent. Phase I has an **AB·B** rhenium stacking sequence in the *c*-direction, where the · symbol is used to indicate where the nitrogen is positioned between the rhenium layers. This phase has three metallic layers and one nitrogen layer, for a 3:1 rhenium to nitrogen ratio, or Re_3N as the stoichiometric expression. The phase II proposed by Friedrich has an **A·AB·B** stacking sequence in the *c*-direction. This phase has four metallic layers with two nitrogen layers, for a 4:2 rhenium to nitrogen ratio, or Re_2N. In a different study, Li and Zeng introduced a NiAs-like ReN structure by means of ab initio calculations [10]. This last structure consisted of **A·A·** layers, a metallic layer with a nitrogen layer, or a 1:1 compositional ratio. They reached the conclusion that such a structure is highly probable because of its lower energy compared with other structures of the same composition. All previous structures exhibit a lamella of nitrogen located between layers of rhenium. In this context, a lamella is a mono-atomic hexagonal layer of nitrogen.

With this prior evidence in mind, it is worth considering two possible pathways of nitrogen absorption into a rhenium matrix. The traditional interstitial solid solution is governed by an **ABC** rhenium stacking sequence because ReN_x gives fcc structures where nitrogen occupies the interstitial sites at random. The non-traditional solid solution is guided by localized structural modifications to the parent metal, i.e., a dislocation of stacking planes where nitrogen is located just below the slipped plane in the stacking sequence. Can we still consider this type of compound a solid solution, as the structure of the parent metal has changed only in a small fraction of the entire volume? The 6-coordinate nitrogen atoms in this situation are coordinated to rhenium neighbors in trigonal-prismatic sites. We hypothesize that for any possible composition, the absorption of nitrogen in rhenium causes a stacking fault (or the sliding of one plane) for the next rhenium layer. Using

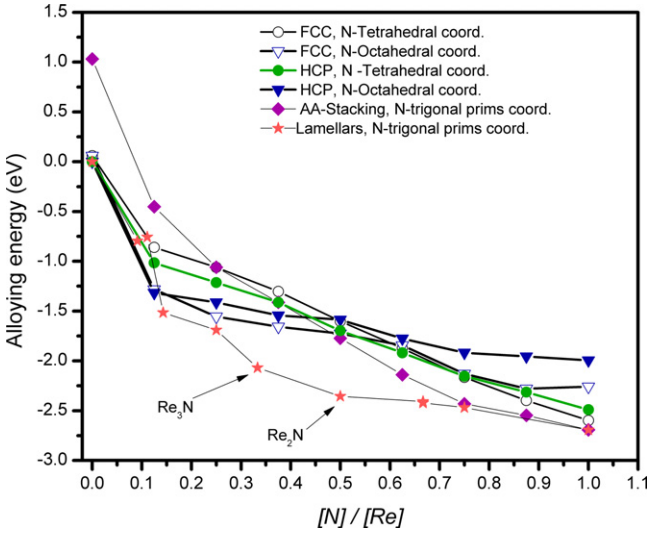

Fig. 1. Alloying energy, as defined in the text, versus nitrogen content.

this hypothesis, it is possible to propose a number of nitrides with varying nitrogen contents. The operating rule is that a stacking fault of the metal layer is generated when a complete nitrogen layer is below it. Following that rule, **AB·B**, **A·AB·B**, **ABA·AB**, **AB·BA·AB**, **ABAB·BAB**, **A·A·AB** and **A·A·** are valid compounds, with 3:1, 4:2, 5:1, 6:2, 7:1, 4:2 and 1:1 compositional ratios, respectively. Thus, a single composition may have several non-equivalent stacking sequences. The Re_3N and Re_2N phases proposed by Friedrich are contained within this set of hypothetical compounds.

3. Cohesive energy calculations of the interstitial and lamellar structures

We have performed a comparative analysis of the traditional interstitial solid solutions versus the layered solid solutions with the aim of elucidating their relative stability. The criterion used to establish which structure has a better stability is the alloying energy, defined by Eq. (B.1) (see Appendix B). This equation uses as points of reference the energies of hcp metallic rhenium and atomic nitrogen. Negative values signify stability toward spontaneous dissociation, but not to the formation of other possible phases. To take into account structural variations as broadly as possible for the interstitial solid solutions, we performed several series of calculations that preserved the structure of the parent metal under increasing nitrogen contents. The first series, for the fcc N-tetrahedral sites (the open circle in Fig. 1), uses as a starting point the structure of rhenium in a face-centered cubic arrangement; the nitrogen atoms sequentially fill the tetrahedral interstices. The $x = N/Re$ ratio is given by the number of occupied interstices. The second series, for the fcc N-Octahedral sites (open triangle in Fig. 1), correspond again to the prototypical rhenium in a face-centered cubic structure, but here nitrogen fills the octahedral interstices. For the above two series the "cubic" term must be viewed with caution because the symmetry of the structure has been reduced to that of a rhombohedral system. In the rhombohedral representation, we performed volume and c/a cell optimizations. When the resulting c/a ratio is not the ideal ratio of 1.633, then the optimized structure cannot be considered cubic. We use "cubic" to designate the prototypical rhenium structure. The third and fourth series are similar but have rhenium in an hcp configuration, given by closed circles and triangles for the tetrahedral and octahedral nitrogen sites, respectively. The fifth series uses rhenium in a fixed **AA** stacking, represented in the figure by filled rhombs. Nitrogen occupies trigonal prism sites. At $x = 1$, this series gives the NiAs-like ReN

structure reported by Li and Zeng [10] as the most stable polymorph of rhenium nitride. When $x < 1$ some of the trigonal prism sites are empty, and thereafter that series can be considered a nitrogen deficient NiAs-like ReN_x. All of the above structures comply with the main clause for an interstitial solid solution. That is, the structure of parent metal is (nearly) maintained while nitrogen fills the interstitial spaces. We have generated the nitrogen filling in a pseudo-random pattern (see Appendix C). The sixth series is for lamellar compounds. For this series we planned several prototype structures following the rule of the stacking fault, as indicated in the preceding paragraph. Again, at $x = 1$, this series gives the NiAs-like ReN structure as the only solution. The details of the supercell creation for the above series are given in Appendix C. The important results of this study are summarized in Fig. 1 according to the alloying energies. The reaction of rhenium with nitrogen is exothermic when starting from nitrogen in the atomic state. This may not be true for nitrogen in the molecular state. It is significant that in the $0.2 \leq x \leq 0.7$ range of compositions, the lamellar compounds are, without doubt, superior in stability compared with any of the other possibilities. They are always energetically favored by a wide margin over the interstitial dissolutions. For $x \leq 0.1$ the results are unclear. Apparently, in this composition, the interstitial dissolutions are of higher stability. However, it must be considered that the supercells needed to give these compositions are quite large for the lamellar type, and thus the error of the calculations could obscure the real trend. For $x \geq 0.7$, the nitrogen deficient NiA*s*-like rhenium nitrides are almost as stable as the lamellar prototypes. However, the lamellar compounds are still favorable by a very small margin.

4. Diffractograms for the calculated structures

Each of the structural variations in Fig. 1 was optimized according to the best canons of ab initio calculations. That is, the optimization of the volume, *c*/*a* and internal atom coordinates (when possible) were performed. From the structural data, we can generate diffraction patterns for any nitrogen concentration. Fig. 1 shows that the hcp arrangement will be energetically surpassed by an equivalent fcc system except for systems with very low nitrogen concentrations, where $x < 1/8$. For that reason, the simulated diffractograms of those series will be not presented here. However, the trends for the hcp-based interstitial solid solutions are comparable to those of the cubic systems regarding the evolution of their diffractograms.

4.1. Diffractograms for nitrogen in octahedral interstices in a pseudo-cubic rhenium matrix

Fig. 2 shows a hypothetical sequence of diffraction patterns for the incorporation of nitrogen in the octahedral interstices of rhenium in an fcc structure. This sequence is the second most stable arrangement according to the calculated energies for $x < 0.5$ (the open triangles in Fig. 1). There is a uniform expansion of the unit cell for $x < 5/8$; that is, the cubic symmetry is retained. However, for $x \geq 5/8$, the energy is further minimized when the structure is allowed to elongate in the {1 1 1}-direction; that is, the cubic symmetry is lost. The diffraction peaks separate due to the broken symmetry along the main crystal axes. Importantly, the cubic symmetry for rhenium with nitrogen in the octahedral interstices is unstable only with a high nitrogen content. There is a threshold point at $x \sim 5/8$; below that composition, the crystalline system can be cubic, while it is trigonal for higher compositions. In another report, tetragonal distortion is also considered [5]. Nevertheless, the high concentration of nitrogen in this arrangement is highly unlikely due to the high alloying energy, shown in Fig. 1, which was more positive than some of the other series calculated.

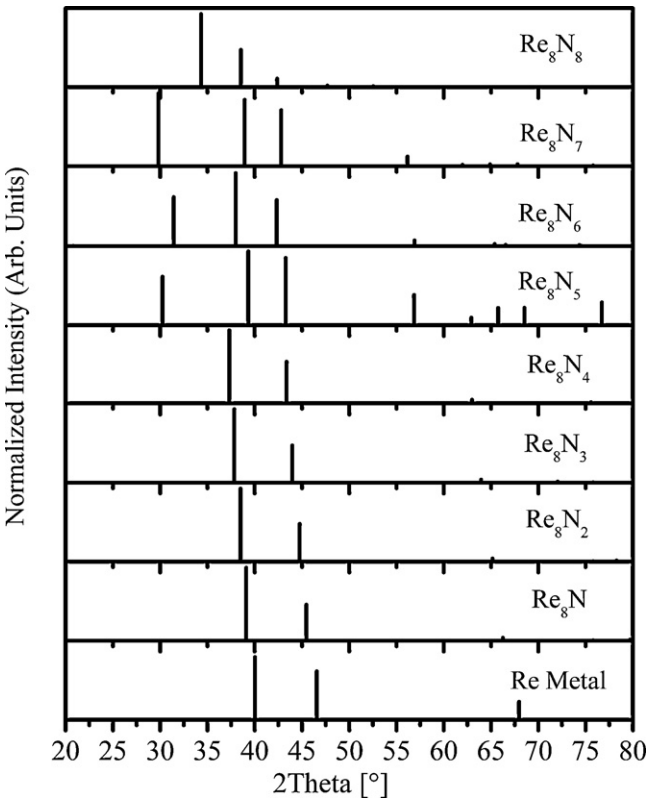

Fig. 2. Diffraction patterns from numerical simulations, in which the nitriding of rhenium occurs by nitrogen dissolution in octahedral interstices in a cubic face-centered rhenium structure.

4.2. Diffractograms for nitrogen in tetrahedral interstices in a pseudo-cubic rhenium matrix

Fig. 3 is an analogous sequence of diffractograms starting from rhenium in an fcc structure, but here the nitrogen atoms fill the tetrahedral interstices. This sequence corresponds to the filled triangles in Fig. 1. The cubic structure is mechanically unstable at the middle of the range of compositions, that is, when $3/8 \leq x \leq 5/8$, where the trigonal distortions of the cubic symmetry have lower energies. In the computer-generated diffractograms, the peak from the (1 1 1)-planes of the cubic system is split due to this distortion. As seen in the diffractogram, the splitting of peaks is less prominent than in the case of octahedral interstices, indicating that the trigonal distortion is more minor in scale than in the above case. The calculated alloying energies indicate that this series will be implausible for low nitrogen concentrations but will become feasible for $x \sim 1$. This can be explained by the distortion required to accommodate nitrogen in the tetrahedral sites. At small concentrations the gain in energy upon the introduction of nitrogen does not fully compensate for the energy required to expand the cell volume of the metal structure. At $x \sim 1$ the metal structure has already been expanded, making the tetrahedral sites larger and energetically favored over the octahedral sites. The tetrahedral site occupancy is at an advantage over the octahedral sites for $x > 6/8$.

4.3. Diffractograms for nitrogen in trigonal prismatic sites in an ***AA***-stacking sequence of rhenium atoms

Another interesting series is generated when nitrogen atoms fill the trigonal prism sites in rhenium characterized by **AA**-stacking. Evidently, at low nitrogen concentrations, this structural arrangement is highly improbable because the compound has positive energies in comparison with other variants of the same

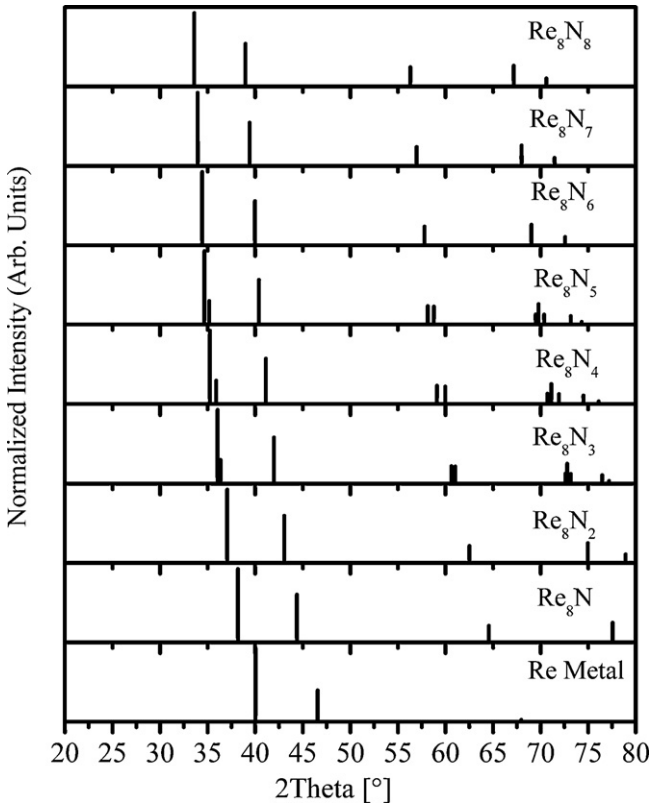

Fig. 3. Diffraction patterns from numerical simulations, in which the nitriding of rhenium occurs by nitrogen dissolution in tetrahedral interstices in a cubic face-centered rhenium structure.

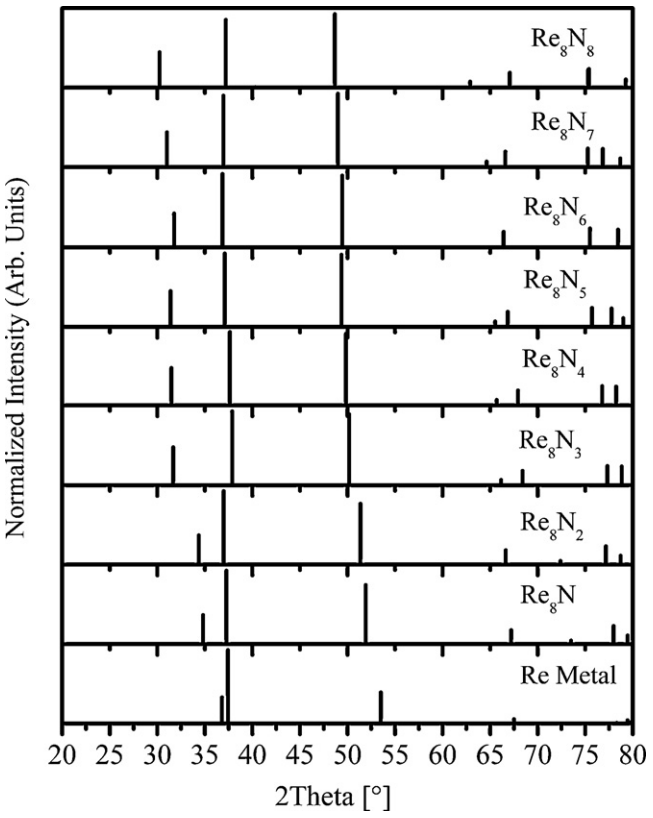

Fig. 4. Diffraction patterns from numerical simulations, in which the nitriding of rhenium occurs by nitrogen dissolution in trigonal prism sites in an AA stacking sequence of rhenium atoms.

composition (Fig. 1). However, as with the nitrogen concentration augment, this arrangement becomes physically feasible because of their negative energies. In fact, this is the second most probable arrangement for $x > ½$, and asymptotically, their energies make contact with the sequence of lamellar structures. Their diffractograms are given in Fig. 4. As the nitrogen concentration increases, the cell volume expands and their characteristic distances also enlarge. This is visualized in this sequence of diffractograms by the migration of peaks to lower angles. As the distances between the *c*-planes are affected more rapidly than the distances between the basal planes, the peaks associated with the (0 0 *) Miller indices move faster than the peaks for the (0 * 0) indices.

4.4. Diffractograms for nitrogen–rhenium lamellar compounds

Fig. 5 shows a sequence of diffraction patterns when nitrogen is incorporated in rhenium, under the assumption that the incorporation will occur through a lamellar dissolution. What we see in Fig. 5 brings to mind the general trend of a solid solution: a gradual transformation of a fundamental structure. However, unlike a traditional solid solution, where the metal structure expands (nearly) evenly in all directions, here the structure widens more rapidly in the *c*-direction, maintaining the interatomic distances in the basal plane somewhat unchanged. To clarify this point, we have indexed the patterns of nitrides in association with the main diffraction peaks of the parent metal. The symbol (0 * 0) stands for diffraction due to distances in basal plane. The symbol (0 0 *) indicates diffraction peaks due to the interplanar distances in *c*-direction. The (0 * *) diffraction develops from a family of planes that bisect the cell of the parent metal, as shown in Fig. 6(a). These planes remain in the lamellar compounds as the nitrogen content increases, as shown in Fig. 6(b) for $Re_{11}N$ and Fig. 6(c) for ReN. When the periodic arrangement

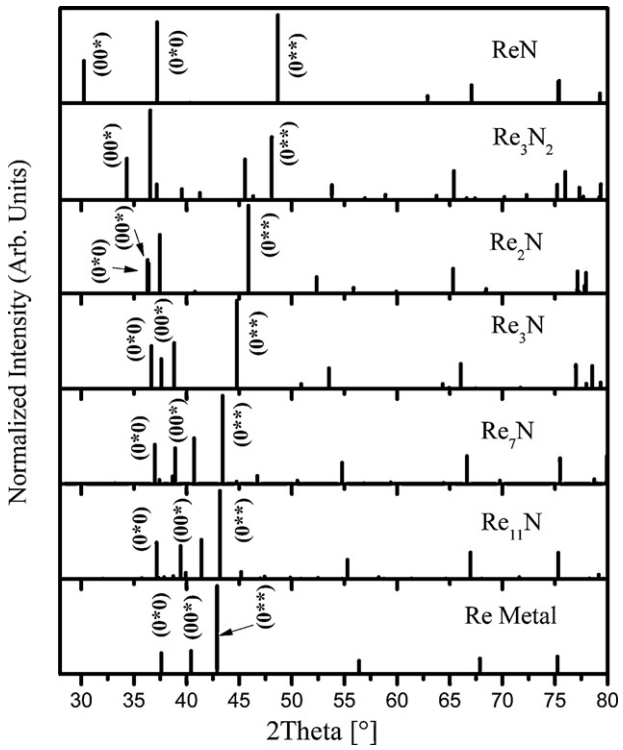

Fig. 5. Diffraction patterns from numerical simulations, in which the nitriding of rhenium occurs by means of lamellar dissolution.

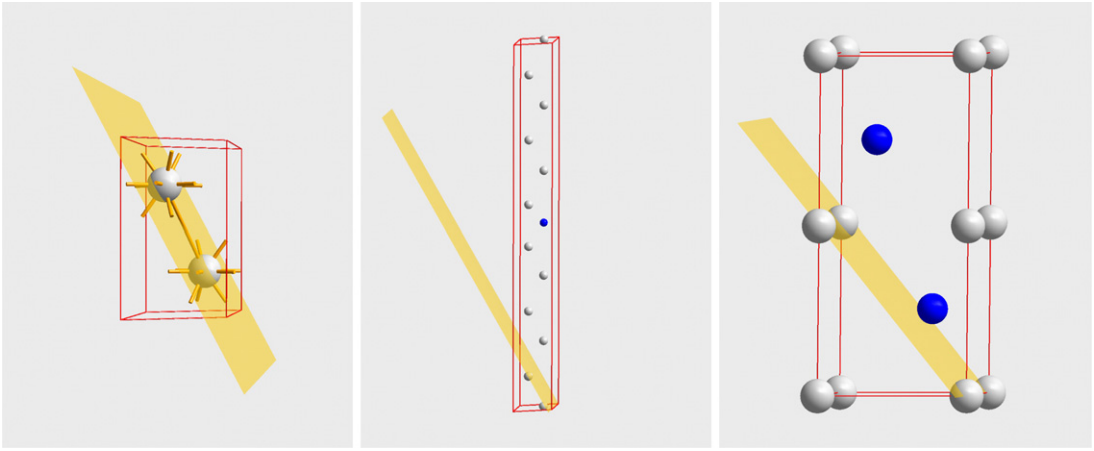

Fig. 6. (0**) planes in three different unit cells that produce equivalent diffraction peaks: (a) in metallic rhenium, (b) in $Re_{11}N$ and (c) in NiAs–ReN.

of any plane is disrupted, as happens in the $Re_{11}N$ pattern for the (0**) planes, the corresponding diffraction peaks split into several satellite peaks. Although this plane is defined by the Miller index (0 1 1) in the pure metal cell, the equivalent plane is defined by the Miller indices (0 1 6) in the $Re_{11}N$ cell (Fig. 6(b)) and (0 1 2) in NiAs–ReN (Fig. 6(c)). It should be noted that indexing to the true Miller indices might be meaningless because the cell of reference is changing. In Fig. 5, we see that the (0**) diffraction moves to higher angles, meaning that these planes are growing closer in a perpendicular direction. In contrast, the (00*) diffraction moves from 40.4° in metallic Re to 30.2° in NiAs–ReN. At the same time, the (0*0) diffraction remains almost immobile, changing only from 37.6° in Re to 37.2° in NiAs–ReN. To understand this behavior, we must analyze the atomic arrangement, the distance between neighbors and the volume occupied by each atom of metal. In metallic rhenium, the mean distance between the Re atoms is 2.750 Å (coordinated to 12 Re neighbors), while in NiAs–ReN the mean distance is 2.828 (coordinated to 8 Re neighbors). At the same time, the specific volume (i.e., the volume occupied by a single Re atom) changes from 14.70 $Å^3$ for metallic Re to 19.89 $Å^3$ for NiAs–ReN. This represents a 35% volume expansion to accommodate nitrogen atoms; evidently the expansion occurs due to a greater separation between the metal neighbors. Indeed, the basal in-plane metal-to-metal distances remain nearly the same. For instance, the Re–Re in-plane distance is 2.760 Å in metallic Re, while it is 2.789 Å in NiAs–ReN. This means that most of the volume expanse is at the expense of the out-of-plane distances. On average, these distances are becoming longer. That explains why the (00*) diffraction changes significantly, whereas the diffraction (0*0) remains nearly at its original value. In conclusion, the volume needed to accommodate the nitrogen atoms in this kind of lamellar dissolution is obtained by a greater separation of the planes in the *c*-direction.

5. The deposition of rhenium nitride films by reactive sputtering

In the past, we have prepared rhenium nitride films by the pulsed laser deposition method [4]. Now, we will focus on the structures of the films produced by sputtering. The experimental setup and method for film preparation are described in Appendix A. To demonstrate the successful synthesis of rhenium nitride by this method, Fig. 7 shows a representative Auger spectrum of a deposited film. It exhibits mainly rhenium and nitrogen, although some traces of oxygen are also detected. This particular film was produced after sputtering a rhenium target under a flow of nitrogen with $F_N = 20\,mL\,min^{-1}$. The films are homogeneous in composition along the substrate surface. Fig. 8 shows selected XRD patterns for the rhenium nitride samples grown at different nitrogen flow rates. Because the deposition rate is very low, these films are grown over the course of 50 min. The Si substrate has peaks at 28.40° (1 1 1) and 58.85° (2 2 2), indicated with a * symbol in Fig. 8. The pure Re sample, deposited with $F_N = 0$, shows three main diffraction peaks at 37.51°, 40.4° and 42.8°. These correspond to the diffraction planes (1 0 0), (0 0 2) and (1 0 1), respectively, of the hexagonal close packed structure reported in the powder diffraction file (PDF) #89-2935. However, it shows (0 0 2)-Re to be preferentially parallel to the (1 1 1)-Si crystalline growth. For the $F_N = 16\,mL\,min^{-1}$ sample, the hexagonal Re peaks were not present. Instead, wider peaks at approximately 38.44° (A), 44.69° (B), 65.20° (C) and 78.1° (D) appear in the pattern. This phase can be indexed to an fcc rhenium nitride phase, as reported by Fuchigami et al. [5], with $a_o = 4.03 \pm 0.03$ Å. For higher values of F_N, the positions of peaks A through D shift to lower angles as the N/Re ratio in the films increase. The shift is more noticeable for peak A. It shifts to 38.16° and then to 36.46°. These shifts indicate that the crystalline structure is expanding with increasing nitrogen content. Additionally, the intensities (relative to that of peak A) of the B, C and D peaks decrease for $F_N = 20\,mL\,min^{-1}$ and then are not present for the $F_N = 30\,mL\,min^{-1}$ sample, indicating the loss of long-range symmetry in their respective crystalline directions. For the

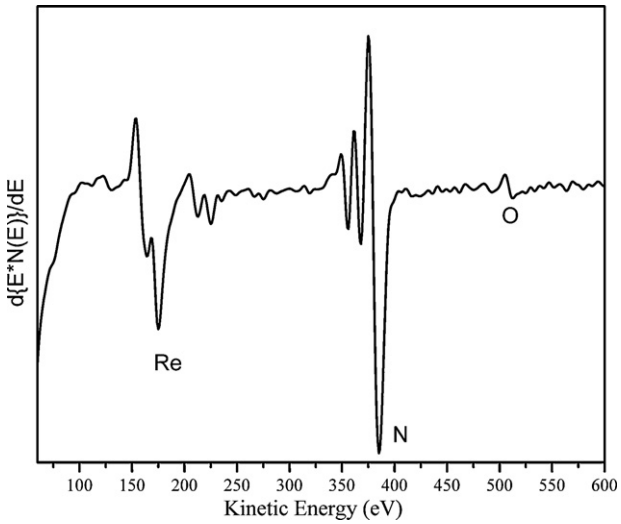

Fig. 7. Auger spectrum of a film produced by magnetron sputtering of a rhenium target with $P_N = 80$ mTorr.

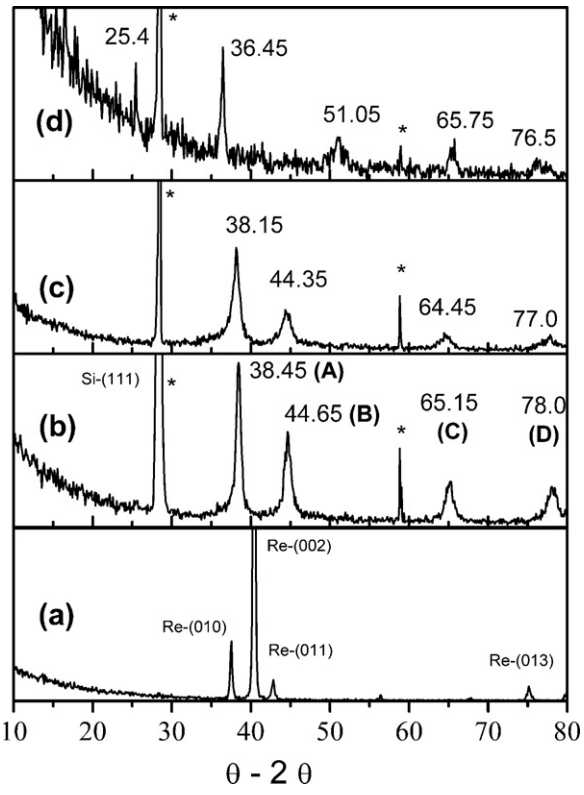

Fig. 8. XRD patterns for selected films: (a) $F_N = 0$; (b) $F_N = 16$; (c) $F_N = 20$; (d) $F_N = 30\,mL\,min^{-1}$. The best match with the series fcc rhenium N-octahedral sites is (b), $x \sim 0.25$. For $F_N = 20$ the composition is within $0.25 \leq x \leq 0.375$ with N in octahedral sites.

$F_N = 30\,mL\,min^{-1}$ sample, two new broad peaks appear at approximately 51.02° (E) and 65.44° (F), which may be related to a different phase of rhenium nitride, given its wide shape. However, no phase in the PDF database or reviewed literature for rhenium in metallic, nitride or oxide forms was found that agreed with those two peaks. In the same sample, new peaks were present at 16.45° (1 1 0) and 25.47° (2 1 0), which might be indexed to a hexagonal crystalline phase of ReO_3 using PDF #40-1155.

6. Discussion

The calculations provide evidence that the reaction between nitrogen and rhenium is facile, as long as the reaction begins with atomic nitrogen, as it is always exothermic (negative energies). This is corroborated by our sputtering experiments, where rhenium nitride films were deposited without difficulty, although with a very low deposition rate. The diffractograms allow us to compare the theory and the experiments. The best agreement of the deposited films is with the series of fcc rhenium N-octahedral sites. For instance, the computer-generated diffractogram for Re_8N_2, N-octahedral, has its main peaks at $\theta - 2\theta$ angles of 38.48° (38.45° experimental), 44.75° (44.65°), 65.14° (65.14°) and 78.3° (78.0°). This small deviation from the experiment is reasonable because the film is attached to a substrate, where residual stresses remain. This experimental pattern can also be adjusted for Re_8N, N-tetrahedral. However, at that composition, tetrahedral nitrogen is implausible because of its higher energy compared with the octahedral nitrogen site. From the close match between the theory and the experiment, it is possible to affirm that the film prepared at $F_N = 16\,mL\,min^{-1}$ has an N/Re ratio in the vicinity of 0.25, and the film produced at $F_N = 20$ mTorr has an N/Re ratio higher than 0.25 but lower than 0.375. The most likely configuration is with nitrogen in the octahedral sites. The film prepared at $F_N = 30$ mTorr does not belong to this structural class of nitrides. Its diffraction at 36.45° is well below the possible diffraction angles for a cubic arrangement. From the experimental X-ray diffraction patterns presented here, several deductions can be made regarding the deposition of rhenium nitride films. First, the metal structure transforms from a hexagonal symmetry to a cubic symmetry when nitrogen is incorporated into the rhenium lattice. Second, our films deposited by reactive DC-sputtering are analogous to those deposited by Fuchigami et al. [5] by means of laser ablation. Third, the cubic structure remains cubic for relatively large variations in the composition, as has been reported in the literature [5–8]. In this case, the interstitial solid solution model appears to be correct. Fourth, as the nitrogen incorporation exceeds a certain value, the cubic symmetry is destroyed and replaced by an unidentified lower-symmetry crystalline system. Fifth, the structures of the sputtered films do not coincide with the phases produced by the high-pressure high-temperature method.

This last statement begs an important question: why are cubic interstitial compounds produced by plasma methods, while the high-pressure and high-temperature methods produce different compounds? As calculations show, neither the tetrahedral sites nor the octahedral sites are the best location for nitrogen in a matrix of rhenium; both tend to distort the interstitial site. The best configuration, in terms of its energy, is the trigonal prismatic site. However, this site does not exist in the base structure. Its creation requires a structural reorganization. The high-pressure high-temperature method is very interesting in this regard [14]. The high temperatures lead to high mobility in the nitrogen atoms, while the high pressure can produce slip planes. The slipped planes produce non-intrinsic trigonal prism sites. Those sites can be stabilized by a group of nitrogen atoms acting collectively that migrate to the adjoining area. The pressure and temperature can be subsequently removed, and the slipped structure will remain because it has been already stabilized. We can consider the high-pressure high-temperature method as a system near its thermodynamic equilibrium. This is because all the species involved in the reaction are given time to reach the best locations, and consequently the compound attains its minimum energy. This process is appropriate for the production of lamellar rhenium nitrides. We are convinced that the Re_2N and Re_3N phases proposed by Friedrich are two particular compositions of this class of compounds. When a complete structural reformation is not possible, the calculation shows that second best arrangement is the traditional interstitial solid solution. Comparatively, the plasma methods are out of equilibrium because the sputtered species contain high kinetic energies, while the substrate remains close to room temperature. The arriving species in ablation or sputter experiments have only a short time to find the appropriate structural arrangement before they thermalize to the substrate temperature. After that, they should remain nearly frozen at those positions at temperatures close to ambient. That is, the rearrangement is limited by the diffusion of nitrogen into rhenium and by the mobility of rhenium. From this perspective, the formation of layered compounds is restricted by the reaction kinetics of the plasma methods. The nitrogen atoms need to form a full nitrogen layer before the arrival of new rhenium species to shape a layered structure. This seems to be impossible given the way that the films are grown by the plasma methods, where all the growing species arrive simultaneously. Following this reasoning, the plasma methods can produce metastable structural arrangements, while the high-pressure and high-temperature methods must produce stable arrangements. However, the transformation of one class of compound to the other class should be possible by thermal treatments at atmospheric pressure, provided that the phase transformation temperature is below the rhenium–nitrogen dissociation temperature.

An interesting topic resulting from this work is the existence of an unusual kind of interstitial dissolution. The traditional interstitial solid solution is formed by a gradual alteration of the base structure using the intrinsic interstices. The transformation is typically an expansion needed to make room for the interstitial atom. The new type of interstitial solid solution requires the use of non-intrinsic interstitial sites. For instance, an hcp metal has a stacking sequence in ABABABAB order. If there is a stacking fault for any reason, the result will resemble ABABAABAB. If nitrogen is inserted into that solid, it will become ABABA·ABAB. While the defect is very unstable without nitrogen, in the presence of nitrogen it becomes stable. Nitrogen is absorbed without affecting the parent metal structure, with the exception of passivating a defect that was previously created. The structural reformation required for this type of nitrogen dissolution is not as great as one might think. This can be seen in the gradual evolution of the diffractograms shown in Fig. 7. Even if the description of the whole structure can be represented in different space groups for minimal differences in composition, the basic structure remains (nearly) unchanged in all compositions. Reviewing the Inorganic Crystal Structures Database (ICSD) for tungsten nitride, as an example, we found many arrangements that might belong to this class of solid solutions. ICSD #76527 (WN), #76005 (WN), #30374 ($W_{2.56}$ N_4), #60193 ($W_{1.1}N$), #60183 ($W_{4.6}N_4$) and #43607 ($W_{0.6}N$) are sample structures that use non-intrinsic sites to accommodate nitrogen. One interesting aspect of this kind of compounds is the apparent polymorphic character. For a certain composition, there will be many structures of the same energy and therefore of the same stability. This reasoning may be pushing the concept of interstitial solid solutions to its limits, but this undeniably a solid solution, where nitrogen uses non-native interstitial spaces. We propose that the old concept must evolve to accommodate a new type of solid solutions discovered with the elapse of time. After all, this concept is already applied to materials that are not solid solutions, including most transition metal nitrides.

7. Conclusions

We have presented here systematic first principles calculations of rhenium nitrides as a function of composition in a variety of possible structural arrangements. The calculations show that neither the tetrahedral sites nor the octahedral sites are the best place to locate nitrogen in a rhenium matrix. The best location is the trigonal prismatic site. This configuration requires non-intrinsic sites in the metallic matrix that must be created. This class of arrangement produces lamellar structures, where nitrogen lamellas (atomic monolayers) are inserted among multiple rhenium layers. The Re_3N and Re_2N phases belong to this class. However, many compositions and structures are possible, where the composition is given by the ratio of the nitrogen layers to the rhenium layers. While the first principles calculations point to higher stability for the lamellar structures, the experimental evidence shows that both the interstitial and the lamellar classes are synthesizable. In fact, our analysis shows that the rhenium nitride deposited by sputtering adopts an fcc N-octahedral structure. We conclude that rhenium nitrides exhibit polymorphism. As such, this new type of lamellar compounds is very interesting. While transition metals intercalated in layered materials such as graphite or MoS_2 are not new, the inverse, layers of nitrogen [6] or carbon [15] interspersed in the transition metal, is seen as a new area worthy of exploration.

Acknowledgments

We appreciate the technical assistance from C. Gonzales, V. Garcia, D. Dominguez and R. Chavez. Financial support from CONACYT grant #82984 is acknowledged.

Appendix A. Experimental methods

Rhenium nitride films were grown by reactive DC-sputtering. The experiment was carried out in a custom made ultra-high vacuum (UHV) deposition system. The system consists of three stainless steel chambers: sample loading, deposition and analysis. The analysis chamber is a PHI-548 apparatus equipped with X-ray photoelectron (XPS) and Auger electron (AES) spectroscopies, and it operates at 10^{-10} Torr by means of an ion pump. The sample loading and deposition chambers are independently evacuated to 10^{-8} Torr or better by a 130 L s^{-1} turbomolecular pump. A 2.5 cm diameter Re target (99.9%) was positioned in a magnetron gun, 10 cm above a (1 1 1)-silicon substrate. A mechanized rod is used to transfer the sample between chambers, which are isolated by gate valves. With this setup, the deposited films can be analyzed without exposure to the outside atmosphere. The rhenium nitride films were deposited at room temperature at different N_2 pressures in the following manner. In the deposition chamber, a mass-flow controller fed N_2 (ultra-high purity grade) at increasing flows to set pressures ranging from 3 mTorr (1 mL min^{-1}) to 180 mTorr (35 mL min^{-1}). After setting the N_2 pressure, an additional 5 mL min^{-1} of Ar (ultra-high purity grade) was allowed into the chamber. The samples were grown at 120 W for 50 min and were then immediately transferred to the analysis chamber. A reference sample, metallic Re, was deposited in the absence of N_2. The assessment of nitride formation was performed by comparative core-level energy shifts in the XPS in relation to the metallic Re sample. The XPS measurements used an Al K-α ($h\nu$ = 1486.6 eV) X-ray non-monochromatic line. The X-ray diffraction (XRD) patterns were collected ex situ in a Philips X'pert diffractometer using the Cu Kα line with λ = 0.154 nm.

Appendix B. Calculation methods

All calculations were performed within the framework of the density functional theory (DFT). We employed the full potential linearized augmented plane wave (FP-LAPW) method, as implemented in the Wien2k code [16]. The exchange and correlation effects were treated using the generalized gradient approximation, as given in [17] and [18]. We used muffin-tin radii of 1.8 au for Re and 1.3 au for N and angular momenta up to l = 10. We were committed to approximately 47 k points in the irreducible part of the Brillouin zone for each of the evaluated supercells. This is trivial for the interstitial phases because they preserve the number of metallic atoms, as shown in Table I. However, for the lamellar structures, the number of k points was varied to compensate for the dissimilar cell volumes required for the different compositions. To compare the relative stability of several crystalline phases, we use as point of reference the energy of the bulk rhenium cell in its basal hexagonal state, $E^{\mathrm{Tot}}_{Re\text{-bulk}}$, which is calculated using the same level of accuracy and parameters. The energy of each individual nitrogen atom was calculated considering a cubic supercell (fcc-box) that contains such an atom. The fcc-box lattice was held constant to 25 Bohr and identical RMT and RKMAX as in rhenium nitride compounds. The energy of the isolated nitrogen atom is then $E^{\mathrm{tot}}_{\mathrm{N}}$. The alloying energy is calculated from the total energy of the i-cell, $E^{\mathrm{Tot}}_{\mathrm{i}}$, minus the energy of n atoms of rhenium, minus the energy of m atoms of nitrogen. To compare the energies of cells with different volumes where the number of enclosed atoms varies, it is preferable to use the energies per atom. Thus, the alloying energy is calculated according to the following formula, as it was defined in Ref. [19]:

$$E^{\mathrm{alloy}}_{\mathrm{i}} = \frac{E^{\mathrm{Tot}}_{\mathrm{i}} - nE^{\mathrm{Tot}}_{Re\text{-bulk}} - mE^{\mathrm{tot}}_{\mathrm{N}}}{m+n} \tag{B.1}$$

Here n and m are the number of rhenium and nitrogen atoms, respectively, contained in the volume of the i-cell.

Table I
Steps to reduce the symmetry of prototype cell, in this case for cubic and hexagonal structures with octahedral interstices.

Cubic cell transformation			Hexagonal cell transformation		
1	2	3	1	2	3
Base group: *Fm3m*	Doubled cell group: *Fm3m*	Reduced cell group: *R−3m*	Base group: $P6_3/mmc$	Double cell: $P6_3/mmc$	Reduced cell group: *P−3m1*
Axes: $x=y=z=a$ $\alpha=\beta=\gamma=90^\circ$	Axes: $x=y=z=2a$ $\alpha=\beta=\gamma=90^\circ$	Axes $x'=\frac{1}{2}y+\frac{1}{2}z$ $y'=\frac{1}{2}x+\frac{1}{2}z$ $z'=\frac{1}{2}x+\frac{1}{2}y$ $\alpha=\beta=\gamma=60^\circ$	Axes $x=y=a$, $z=c$ $\alpha=\beta=90^\circ$ $\gamma=120^\circ$	Axes $x=y=2a$, $z=c$ $\alpha=\beta=90^\circ$ $\gamma=120^\circ$	Axes $x'=x$; $y'=y$; $z'=z$ $\alpha=\beta=90^\circ$ $\gamma=120^\circ$
Wyckoff Re sites: 4*a*	Wyckoff Re sites: 24*e*, 4*c*	Wyckoff Re sites: 6*h*, 2*c*	Wyckoff Re sites: 2*c*	Wyckoff Re sites: 2*d*, 6*h*	Wyckoff Re sites: 2*d*, 6*i*
Wyckoff N sites: 4*b*	Wyckoff N sites: 4*a*, 4*b*, 24*d*	Wyckoff N sites: 1*a*, 1*b*, 3*d*, 3*e*	Wyckoff N sites: 2*a*	Wyckoff N sites: 2*a*, 6*g*	Wyckoff N sites: 1*a*, 1*b*, 3*e*, 3*f*

Table II
Filling of the Wyckoff positions in the two spatial groups, pseudo-cubic (*R−3m*) and hexagonal (*P−3m1*), to give the different compositions using octahedral sites.

Formula in the unit cell	*R−3m*		*P−3m1*	
	Re Wyckoff positions	N Wyckoff positions	Re Wyckoff positions	N Wyckoff positions
Re_8N_0	6*h*, 2*c*	–	2*d*, 6*i*	–
Re_8N_1		1*a*		1*a*
Re_8N_2		1*a*, 1*b*		1*a*, 1*b*
Re_8N_3		3*d*		3*e*
Re_8N_4		1*b*, 3*d*		1*b*, 3*e*
Re_8N_5		1*a*, 1*b*, 3*d*		1*a*, 1*b*, 3*e*
Re_8N_6		3*d*, 3*e*		3*e*, 3*f*
Re_8N_7		1*b*, 3*d*, 3*e*		1*b*, 3*e*, 3*f*
Re_8N_8		1*a*, 1*b*, 3*d*, 3*e*		1*a*, 1*b*, 3*e*, 3*f*

The accuracy of the DFT calculations is confirmed by the comparison of the cell parameters with the few reported Re–N structures. For instance, the cell parameters for Re_2N in this work are $a=b=2.8547$ Å and $c=9.8667$ Å, while from Ref. [6], the recovered material at ambient conditions gives powder diffraction data with $a=b=2.83$ and $c=9.88$ Å. For Re_3N, the calculated values are $a=b=2.8274$ and $c=7.172$ Å, compared with $a=b=2.8105$ and $c=7.154$ Å, values taken from the same Ref. [6]. For the NiAs-like ReN, we calculated $a=b=2.7887$ and $c=5.9058$ Å, while in Ref. [10], Li and Zeng calculated $a=b=2.7472$ and $c=5.8180$ Å with similar DFT calculations. The bulk moduli and cohesive energies are also comparable with values given in Refs. [6,10].

Appendix C. Supercell strategy

The Wien2k code requires an input structure to make refinements and calculate the total energy [16]. Making changes in the composition requires an appropriate strategy. That involves creating a supercell, i.e., a larger system where local adjustments can be made without affecting the whole crystal. There are many strategies for building such a supercell. To exemplify the procedure, the cubic and hexagonal structures where the interstitial atoms are in octahedral sites can be represented in the *Fm3m* (225) and $P6_3/mmc$ (194) space groups, respectively. In our case, we customized the cells with doubled volumes. The symmetry of *Fm3m* was reduced to that of *R−3m* (166), and the $P6_3/mmc$ was decreased to *P−3m1* (164). In Table I, we reveal the methodology used to construct cells of lower symmetries. In Table II we display the useable stoichiometric points in the $0 \le x \le 1$ interval. The interpenetrating sublattices in the *R−3m* group are identified by 16 Wyckoff positions: 6 *h* and 2*c* for the metallic sublattice, and 1*a*, 1*b*, 3*d* and 3*e* for the nitrogen sublattice. In these positions, it is possible to set 8 Re atoms and 8 N atoms. For the *P−3m1* group, the metallic sites can be represented by the Wyckoff positions 2*d* and 6*i*, while the octahedral interstices are in the 1*a*, 1*b*, 3*e* and 3*f* positions. For the cubic and hexagonal structures where nitrogen is in tetrahedral sites, the same strategy is used. The *F43m* (216) and *P63mc* (186) groups were reduced to *R3m* (160) and *P3m1* (156), respectively. For the representation of the hexagonal layered nitrides, we use the *P−6* (174) space group. Nitrogen was fixed at the 1*d* Wyckoff positions, and the rhenium layers were added as needed to give the projected composition, alternately using the 2*i* and 2*h* Wyckoff positions. For each added layer, the cell was extended in the *c*-direction, and the *z*-coordinate of the 2*i* and 2*h* Wyckoff positions was offset appropriately.

References

[1] O.N. Pierson, Handbook of refractory Carbides and Nitrides, Properties, Characteristics, Processing and Applications, Noyes Publications, New Jersey, 1996.
[2] S.T. Oyama, in: S.T. Oyama (Ed.), The Chemistry of Transition Metal Carbides and Nitrides, Blackie Academic & Professional, London, 1996, pp. 107–120.
[3] G. Soto, M.G. Moreno-Armenta, A. Reyes-Serrato, Comput. Mater. Sci. 42 (2008) 8–13.
[4] G. Soto, A. Rosas, M.H. Farias, W. de la Cruz, J.A. Diaz, Mater. Charact. 58 (2007) 519–526.
[5] M. Fuchigami, K. Inumaru, S. Yamanaka, J. Alloys Compd. 486 (2009) 621–627.
[6] A. Friedrich, B. Winkler, L. Bayarjargal, W. Morgenroth, E.A. Juarez-Arellano, V. Milman, K. Refson, M. Kunz, K. Chen, PRL 105 (2010) 085504.
[7] P. Clark, D. Balamurugan, T. Oyama, Appl. Catal. A: Gen. 184 (1999) 175.
[8] A. Haq ul., O. Meyer, J. Low Temp. Phys. 50 (1983) 123–133.
[9] R.F. Zhang, Z.J. Lin, H.-K. Mao, Y. Zhao, Phys. Rev. B 83 (2011) 060101(R).
[10] Y.-L. Li, Z. Zeng, Solid State Commun. 149 (2009) 1591–1595.
[11] B. Matthias, J. Phys. Chem. Solids 7 (1958) 98.
[12] M.E. Vol'pin, Yu.N. Novikov, N.D. Lapkina, V.I. Kasatochkin, Yu.T. Struchkov, M.E. Kazakov, R.A. Stukan, V.A. Povitskij, Yu.S. Karimov, A.V. Zvarikina, J. Am. Chem. Soc. 97 (1975) 3366–3373.
[13] H. Hahn, A. Konrad, Z. Anorg. Chem. 264 (1951) 174–182.
[14] A. Jayaraman, Rev. Sci. Instrum. 57 (1986) 1013.
[15] E.A. Juarez-Arellano, B. Winkler, A. Friedrich, L. Bayarjargal, V. Milman, J. Yan, S.M. Clark, J. Alloys Compd. 481 (2009) 577–581.
[16] P. Blaha, K. Schwarz, G.K.H. Madsen, D. Kvasnicka, J. Luitz, Wien2k, An Augmented Plane Wave + Local Orbitals Program for Calculating Crystal Properties, Karlheinz Schwarz, Techn. Universität Wien, Austria, 2001.
[17] J.P. Perdew, Y. Wang, Phys. Rev. B 45 (1992) 13244.
[18] J.P. Perdew, K. Burke, M. Ernzerhof, Phys. Rev. Lett. 77 (1996) 3865.
[19] C. Stampfl, W. Mannstadt, R. Asahi, A.J. Freeman, Phys. Rev B 63 (2001) 155106–215116.